

Analysis of BEAVRS Revision 2.0 LWR Whole Core Calculation Using MVP with JENDL-4.0

Motomu Suzuki, Yasushi Nauchi

*Nuclear Technology Research Laboratory, Central Research Institute of Electric Power Industry (CRIEPI):
2-6-1 Nagasaka, Yokosuka, Kanagawa 240-0196 Japan, s-motomu@criepi.denken.or.jp*

Abstract - *With the update of the BEAVRS benchmark model, modified points were reflected to whole core models for the MVP code calculation. The initial startup tests of the HZP condition were calculated using the latest beta version of MVP code with the nuclear data library based on JENDL-4.0. The calculation results are discussed through two comparisons. The one is an influence of benchmark model by comparison of revision 1.1.1 and revision 2.0. The other is an effect of code update by comparison of MVP-2 and MVP-3 beta version, including the effect of the resonance scattering model. The update of the benchmark model influences the integral parameters such as effective multiplication factor, control rod bank worth and ITC. The thermal neutron flux distribution evaluated by in-core detector signals is well improved by the update of the benchmark model. Thanks to the tilt-corrected data in revision 2.0, a large discrepancy between calculations and the measured data at the outer of the core region is drastically improved. For the comparison between code versions, the criticality of MVP-3 beta version is slightly lower than MVP-II code. The control rod bank worth, ITC, in-core detector signals and fission reaction distribution vary little with the code updates. From these comparisons, MVP-3 beta version with the exact model has good results. These results indicate that the latest version of MVP can provide accuracy results in HZP condition and contribute verification and validation for MVP-3 code.*

I. INTRODUCTION

A continuous-energy Monte Carlo code MVP [1] developed in Japan Atomic Energy Agency (JAEA), is often used as a reference code in comparison with a deterministic code, an experimental analysis, and a safety evaluation by a regulatory body in Japan. Most studies using the MVP code have focused on lattice/multi-lattice calculations and small core calculations such as for critical assemblies. For a large scale calculation targeting whole core of Light Water Reactor (LWR), only a few studies were reported concerning evaluation of a criticality and a part of the power distribution [2,3]. Recently, a LWR whole core calculation with detailed modeling using BEAVRS (Benchmark for Evaluation And Validation of Reactor Simulations) benchmark was performed in Central Research Institute of Electric Power Industry (CRIEPI) [4]. However, an exact resonance scattering model such as the doppler broadened rejection correction (DBRC) in the MCNP code was not taken into account in the calculation, since the model has not been installed in the published version of the MVP (MVP-II). The exact model with the weight correction method will be installed to the latest version of MVP (MVP-3) as one of new functions [5,6].

The BEAVRS benchmark problem was released by Massachusetts Institute of Technology (MIT) [7]. This benchmark problem provides the most detailed specifications at present to allow a construction of a whole core model for neutronics calculation. The revision 1.0/1.1/1.1.1 benchmark specification were applied to Monte Carlo codes and a deterministic code [8,9,10]. Through comparisons of the calculations to the benchmark

model, a tilt had been indicated in thermal neutron flux map which is evaluated from measured in-core detector signals. The latest version of the benchmark revision 2.0 was released in Sep. 2016 and some specifications including thermal neutron flux map were updated [11].

This paper presents the calculation results of MVP-3 beta version targeting the initial startup tests of the hot zero power (HZP) condition of the BEAVRS revision 2.0. The calculation results are discussed through two comparisons. The one is an effect of benchmark model by comparison of benchmark model between revision 1.1.1 and revision 2.0. The other is an effect of code update by comparison of MVP-II and MVP-3 beta version. This comparison includes the effect of the resonance scattering model. Hereafter, the published version of the MVP (MVP-II) is referred as MVP-2, and the latest beta version of MVP (MVP-3 beta) is also referred as MVP-3b.

II. CALCULATION MODEL AND CONDITION

The BEAVRS benchmark problem describes a detailed information such as the geometry and material specifications to construct neutronics calculation model of commercial Pressurized Water Reactor (PWR) core. The geometric specification consists pin cells, fuel assemblies and the core. Each specification has a horizontal and a vertical geometry. That of pin cell contains fuel pins, burnable poisons, guide tubes, an in-core detector. In addition, upper and lower structure information such as plenum regions, end plugs, an upper and lower nozzles and support plates are also included. The fuel assembly information has positions of burnable absorbers inside guide

tubes and grid spacers. The core loading pattern contains assembly enrichments, insertion of burnable poison rods, and in-core detectors, and control rod cluster assemblies (hereafter, “control rod”) which are categorized into 9 banks. In-vessel structures such as a baffle plate, a core barrel and a reactor pressure vessel are also included. Table I and Table II present the major specifications of the PWR core and fuel assembly, respectively.

The benchmark also describes the operation conditions such as history of the power and the boron concentration for cycles 1 and 2, measurement data for the validation that contains HZP reactor physics tests, and in-core detector signals. The results of reactor physics test contains the criticality boron concentration, the control rod bank worth and the isothermal temperature coefficient (ITC) for some conditions, wherein control rods of some banks were fully

Table I. Major specification of BEAVRS PWR core [11]

Core	
Number of fuel assembly	193
Core power	3,411 MWth
Operating pressure	15.51 MPa
Core flow rate	61.5×10^6 kg/hr
Structure	
Baffle plate material	SUS304
Core barrel material	SUS304
Neutron shield panel material	SUS304
Pressure vessel material	Carbon Steel 508

Table II. Specification of fuel assembly in cycle 1 [11]

Fuel assembly	
Lattice	17x17
Assembly pitch	21.50 cm*
Active fuel length	365.76 cm
Fuel rod pitch	1.260 cm*
No. of fuel rods	264
Fuel rod	
Pellet material	UO ₂
²³⁵ U enrichment	1.6, 2.4, 3.1 wt%
Pellet diameter	0.78 cm*
Cladding material	Zircaloy
Cladding diameter (Inner/Outer)	0.80/0.91 cm*
Control material	
Control rod material	Ag-In-Cd/B ₄ C
Burnable poison material	Borosilicate Glass
No. of burnable poison rods	6, 12, 15, 16, 20
Grid spacer	
No. of grid spacers	8
Grid spacers material for fuel rod	Inconel718, Zircaloy
Grid spacers material for assembly	SUS304, Zircaloy

* rounded values

inserted. The in-core detector signals are axial thermal neutron flux distributions measured by fission chambers inserted into the center of the 58 assemblies in the core. Both the axially-integrated and axial distributions of the thermal neutron flux are reported.

In the revision 2.0 model, some specifications were updated from revision 1.1.1 model. Major update points are modification of the specifications of control rod, burnable poison, upper and lower region.

The calculation model was precisely constructed for the MVP code. Figure 1 and Figure 2 show the calculation model, which was drawn with respect to a horizontal plane and vertical plane by the CGVIEW code that is bundled with the MVP code.

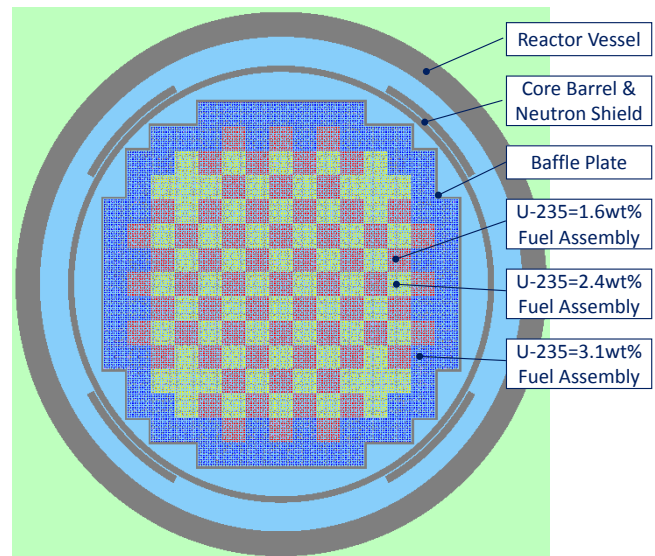


Fig. 1. Horizontal plane of calculation model.

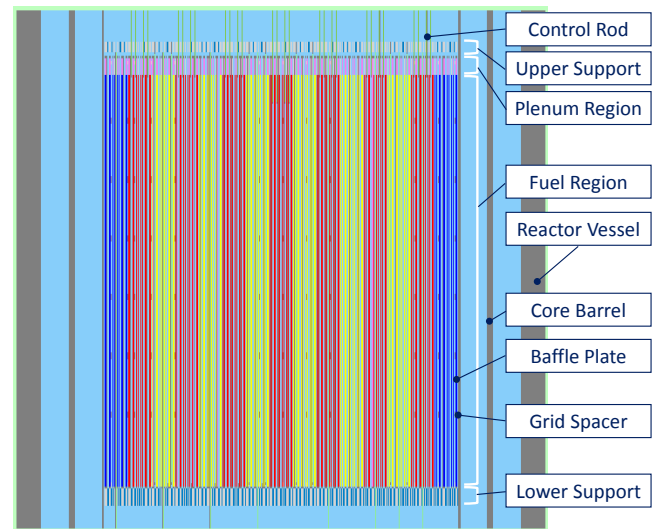


Fig. 2. Vertical plane of calculation model.

III. RESULTS AND DISCUSSIONS

The calculation results are discussed through two comparisons. The one is an effect of benchmark models of revision 1.1.1 and revision 2.0. The other is an effect of code update by comparison of MVP-2 and MVP-3b to clarify the effect of the resonance scattering model. In all of the calculations, a point-wise cross-section library based on JENDL-4.0 was used [12,13]. Parallel calculations with MPI were performed using a Linux cluster owned by CRIEPI, in which each node has two Intel Xeon E5-2670 processors.

In the descriptions of the calculation results, the criteria for the reactor physics tests in ANSI-ANS-19.6.1-2011 standard [14] are used as a reference, although the standard does not address the physics test program for the initial core of a commercial PWR. The criterion for the HZP critical boron concentration is ± 50 ppm, or ± 500 pcm reactivity equivalent. That for the control rod worth for an individual group is $\pm 15\%$, or ± 100 pcm. The ITC criterion is ± 3.6 pcm/K.

1. Comparison of Benchmark Model

To compare the benchmark model between revision 1.1.1 and revision 2.0, each model was calculated using MVP-3b with the exact resonance scattering model. The case of revision 1.1.1 model was evaluated employing 20 billion histories. In the revision 2.0 model, 3 billion histories were used for the criticality and the control rod bank worth, and 15 billion histories were used for the ITC calculation. The standard deviations of revision 2.0 model are slightly higher than revision 1.1.1 model due to mentioned reason. Table I shows the results for the criticality. The benchmark provides the criticality boron concentration in 5 cases wherein control rods of some banks were fully inserted. In the table, the case shows the inserted control rod banks. The boron concentration column shows the measurement data for each case. The calculation result provides the effective multiplication factor in each condition of the control rod banks and the boron concentration in same row. The worth of control rod banks was also evaluated for 7 cases. The results for control rod bank worth are presented in Table II. The results of the criticality and the control rod bank worth for both models can give good accuracy within the criteria. On the other hand, the difference between models have tens pcm, and the difference of the criticality between models are increased with the change of the boron concentration. In the revision 2.0 model, geometries of lower and upper regions of fuel rods were modified. For the burnable poison rods, bottom of active absorber region was defined and end plug was introduced. Upper region of the burnable absorber was also substituted from SUS pin to plenum region. For the control rods, material were updated from only Ag-In-Cd (AIC) to two material combination of B₄C in lower region

and AIC in upper region. Also, the step 0 position of the control rod was shifted to the lower than top of active fuel. Upper and lower region of the control rods were also modified in the same manner as the burnable poison. The difference in the multiplication factor between the models may come from these modifications. Generally, the control rod worth are measured by the boron exchange method, the dynamic rod worth method, etc. In those methods, calculated values of boron reactivity worth and a kinetics parameter are required so that the modification of the benchmark model may affect on the measurement values. However, the reported worth is not varied in the updated benchmark. There is room to study about that.

The isothermal temperature coefficient (ITC) at 566 K was obtained from following equation using the difference in the two eigen-values, which were calculated at 566 K and 572 K since Ref.[14] denote that the increase reactor coolant system temperature in the ITC measurement is a range by 0.6 to 5.6 K. (1 to 10 degree- Fahrenheit).

$$ITC = \frac{\Delta\rho}{\Delta T} = \frac{\rho_2 - \rho_1}{T_2 - T_1} = \frac{(k_2 - k_1)/k_1 k_2}{T_2 - T_1} \quad (1)$$

The ITC calculations considered the changes of the coolant density induced by change in the coolant temperature. The fuel and cladding temperatures for each fuel pins were also changed to match the coolant temperature. Table III shows a comparison of ITC between the calculation results and measurement data. The effect with the model update is small considering the statistical uncertainty in the eigen-value calculations. Both calculation results agree with measurement data within the criteria. However, all of the results have about 2 pcm/K bias from measurement data. The bias has been reported for the revision 1.x model, when a Monte Carlo codes is employed [15]. On the other hand, the results using the deterministic codes does not have the bias [9,10]. Further research including a review of an analysis model and a condition would be required to clarify this difference.

The two thermal neutron flux maps, 2D and 3D maps which were evaluated from in-core detector signals for 58 assemblies are prepared in the benchmark. In the revision 2.0 benchmark, 3D map was slightly modified that the lower regions in the active fuel are increased and the upper regions are decreased. And the tilt-corrected 2D map was also newly added. A tilt-corrected 3D thermal neutron flux map was made from the tilt-corrected 2D data and the original (not corrected) 3D map. The original 3D map was normalized by axial integration of detector signals for each assembly and reconstructed using the tilt-corrected 2D map. In the calculation, the geometry of the detectors was not explicitly modeled. They were estimated with cylindrical tallies whose radius was identical to the inner radius of the gas-filled instrumentation tube. The axial region was divided by 61 points that is consistent with the measurement

data. The bottom of the tallies was located at the same height as the measurement point. The neutron flux inside the tally volume was estimated. Then, by multiplying the flux by the microscopic fission cross section of ^{235}U , the reaction value was estimated. The calculation results were normalized by the sum of all detector signals that were inserted into the 58 assemblies. Fig. 3 shows the comparison of axially-integrated detector signals between the calculation results of MVP-3b and the measurement data. The statistical errors of the calculation are less than 0.2%. In the figure, three values indicate a calculated one using revision 2.0 model, the difference as $(C-E)/E$ between the calculation and the original measurement data (not corrected data), and the difference between the calculation and the tilt-corrected measurement data from top to bottom. The results indicate improvement of the tilt where the upper left region is high and the lower left region is low. For example, the calculation result of revision 1.1.1 at B13 assembly has a large discrepancy about -12% and that is decreased to -1% in the revision 2.0 results. Fig. 4 shows the comparison of the axial distribution at assembly B13. The tilt-corrected experiment data greatly changed from the original data. In the middle of core region, the calculation results of revision 2.0 model gives greater than the results of revision 1.1.1 model.

Comparisons between the calculation results and the measurement data were also evaluated as root mean square (RMS) of following equation.

$$RMS = \sqrt{\frac{\sum_i (E_i - C_i)^2}{N}} \quad (2)$$

Where, i is number of measurement point. Therefore 2D map means axially integrated data of 58 assemblies. 3D map also means 58 assemblies x 61 axial measurement points. Table IV shows RMS for each thermal neutron flux maps. The results of the 2D and 3D map decrease by 3% and 2%, respectively. This variation results from improvement of the tilt in the thermal neutron flux map from revision 1.x to 2.0.

2. Comparison of Code Version

To confirm the effect of calculation code update, the three calculations, (1) MVP-2 with the asymptotic model, (2) MVP-3b with the original scattering model and (3) MVP-3b with the exact resonance scattering model, were carried out using the revision 2.0 model. Hereafter, the asymptotic model is referred as original model, and the exact resonance scattering model is referred as exact model.

The results for the criticality are presented in Fig. 5. In the comparison between MVP-2 and MVP-3b, the results are slightly different. By the comparison between scattering models (MVP-3b with the original model and MVP-3b with

the exact model), it is found that to take the exact model gives smaller effective multiplication factor by tens pcm. In general, introduction of the exact resonance scattering model influences on a resonance absorption reaction of ^{238}U in UO_2 fuel due to considering up-scattering. The pin cell and assembly calculation results were reported that the doppler reactivity increases by 7-10% [16,17]. The difference between the models is due to the effect.

The results for control rod bank worth are also presented in Fig. 6. The deviations with the update are very small and the effect of the exact model does not appear. The control rod bank worth is defined as the difference of two eigen-values. In two calculations, temperature conditions are same. Therefore the effect of the scattering model is canceled out.

The results of ITC were shown in Fig. 7. The results also give the small difference with the update. Unlike a control rod bank worth, ITC is estimated the reactivity corresponding to the change of temperatures. An effect of the exact model should be appeared. ITC consists of a fuel temperature coefficient (FTC) and a moderator temperature coefficient (MTC). These coefficients were calculated for 5 cases varying random number series using revision 1.1.1 model. The history size of these calculations is 20 billion. An average values were evaluated from these results. Fig. 8 shows the calculation results of ITC, FTC and MTC. FTC for each condition have about 3 pcm/K. The effect of the exact model are estimated maximum 0.3 pcm/K from the previous studies [16,17]. However the standard deviations of FTC have a similar value of estimated one. Therefore the effect of the exact model does not appear over the statistical error.

The RMS was evaluated between the tilt-corrected measurement results and the calculation results for each model. Table V shows the results of RMS. The effect of the update of model is small. The effect to thermal neutron flux map between models can be directly compared using pin power distribution. The ratio of fission reaction rate for each pin between the models is summarized for 24 axial nodes in the active fuel region, which is a commonly used value in the neutronics design code. Fig. 9 shows the histogram of the deviation between models using revision 1.1.1 benchmark model. The history size of these calculations is 25 billion. The statistical errors are mainly less than 1.0% around the middle of the core, 2.0% around the outer of the core. In the figure, the results are written regarding lower node 1, 6, 12 that are numbered from the bottom of active fuel, and upper nodes 24, 19, 13 that are axial symmetrical position for the lower nodes. The comparison between lower and upper node, the results have a symmetrical distribution and similar trends in corresponding node. The lower node has a wide distribution, since the statistical errors are increased with shifting to the outer nodes from the middle of the core. Although the almost deviations are within the statistical error, a part of the deviations in the upper nodes are slightly higher than the lower nodes. This

result may indicate that the exact resonance scattering model with the increase of an up-scattering reaction slightly influences not only a capture reaction but also a fission reaction.

Table I. Calculation results of criticality for provided conditions

Case		Calculation result of MVP-3b with exact resonance scattering model		
Insertion condition of Control Rod Bank	Boron Concentration [ppm]	rev. 1.1.1 model (a)	rev. 2.0 model (b)	$\Delta\rho$ [pcm] (b)-(a)
ARO	975	1.00000 ± 0.000004	1.00026 ± 0.000010	27 ± 1
D in	902	1.00167 ± 0.000004	1.00179 ± 0.000010	12 ± 1
C, D in	810	1.00102 ± 0.000004	1.00103 ± 0.000010	1 ± 1
A, B, C, D in	656	0.99957 ± 0.000004	0.99938 ± 0.000011	-18 ± 1
A, B, C, D, SE, SD, SC in	508	0.99810 ± 0.000004	0.99798 ± 0.000011	-12 ± 1

Table II. Comparison of control rod bank worth between calculation results and measurement data

Case	Measurement Value [pcm]	Calculation result of MVP-3b with exact resonance scattering model [pcm]		
		rev. 1.1.1 model (a)	rev. 2.0 model (b)	(b)-(a)
D	788	777 ± 1	787 ± 1	10 ± 1
C with D in	1203	1241 ± 1	1248 ± 1	7 ± 2
B with D, C in	1171	1199 ± 1	1230 ± 1	30 ± 2
A with D, C, B in	548	532 ± 1	517 ± 2	-15 ± 2
SE with D, C, B, A in	461	496 ± 1	473 ± 2	-23 ± 2
SD with D, C, B, A, SE in	772	783 ± 1	791 ± 2	8 ± 2
SC with D, C, B, A, SE, SE in	1099	1112 ± 1	1119 ± 2	7 ± 2

Table III. Comparison of ITC between calculation results and measurement data

Case	Measurement Value [pcm/K]	Calculation results of MVP-3b with exact resonance scattering model [pcm/K]		
		rev. 1.1.1 model	rev. 2.0 model	(b)-(a)
ARO	-3.15	-5.31 ± 0.20	-4.88 ± 0.22	0.42 ± 0.30
D in	-4.95	-7.69 ± 0.20	-7.55 ± 0.22	0.14 ± 0.30
C, D in	-14.42	-16.52 ± 0.21	-16.62 ± 0.24	-0.10 ± 0.32

Table IV. Results of RMS for each measurement data

Case	2D RMS	3D RMS
Revision 1.1.1 model	5.1%	6.6%
Revision 2.0 model	4.8%	6.4%
Revision 2.0 model with Tilt-Corrected Data	1.8%	4.3%

Table V. Results of RMS for each resonance scattering model

Case	2D RMS	3D RMS
Original model	1.8%	4.3%
Exact model	1.8%	4.3%

	R	P	N	M	L	K	J	H	G	F	E	D	C	B	A
1					--	--	0.797 2.6% -2.1%	--	--	0.716 2.4% -1.6%	--				
2			0.694 7.7% -1.2%	--	--	1.267 8.2% 2.0%	--	1.268 3.6% 0.3%	--	--	--	--	--		
3		--	--	--	--	--	--	0.936 4.2% 0.0%	--	0.977 1.2% -0.7%	--	1.197 2.2% 0.2%	--	0.698 1.3% -0.7%	
4		0.936 7.0% -2.2%	1.190 6.7% -0.5%	--	--	--	--	1.163 4.3% 1.4%	--	--	--	--	--	--	
5	--	--	--	--	1.262 8.3% 1.0%	--	--	--	1.164 3.1% 1.8%	--	1.268 1.6% 1.5%	--	1.366 3.4% 4.5%	--	--
6	0.707 5.5% -2.8%	--	0.965 5.0% -1.9%	--	--	1.154 4.8% 1.5%	--	1.077 3.4% 1.2%	--	--	--	--	--	1.267 2.2% 2.0%	--
7	--	--	--	0.957 3.6% -1.8%	--	--	1.029 2.0% 1.7%	--	--	0.904 1.4% 0.8%	--	--	1.205 0.1% 3.2%	--	--
8	0.757 3.6% -2.8%	--	0.927 3.2% -0.9%	--	0.926 1.0% -1.4%	--	0.780 0.8% 0.2%	--	--	1.078 -0.9% 1.3%	--	1.165 -0.9% 1.6%	0.937 -3.0% 0.2%	1.266 -2.2% 0.2%	--
9	--	0.856 2.3% -1.9%	--	--	--	--	--	--	1.031 1.3% 1.9%	--	1.160 -1.3% 1.5%	--	--	--	0.797 -5.7% -2.1%
10	--	--	--	--	0.975 1.1% 0.7%	--	0.899 -2.2% 0.3%	--	--	--	--	1.216 -5.7% 0.4%	--	--	--
11	0.579 0.5% -0.9%	--	--	--	1.263 0.0% 1.2%	--	--	0.931 -3.8% -0.9%	--	--	1.270 -4.5% 1.7%	--	--	--	0.580 -8.0% -0.6%
12	--	--	--	--	--	1.212 -0.9% 0.0%	--	--	0.964 -6.7% -1.1%	--	--	1.324 -7.9% -1.4%	--	--	
13	--	--	0.845 -1.4% -0.8%	--	1.362 1.7% 4.2%	--	--	0.930 -5.5% -0.6%	--	--	--	--	--	0.698 -11.9% -0.6%	
14	--	--	0.694 -0.8% -1.2%	--	--	--	0.860 -6.5% -1.5%	--	--	1.265 -6.8% 1.8%	--	0.943 -10.3% -1.6%	--	--	
15	--	--	--	--	0.581 -3.4% -0.4%	--	--	0.762 -8.9% -2.0%	--	--	--	--	--	--	

Calculation results		
C/E-1 [%] using original measurement data		
C/E-1 [%] using tilt-corrected measurement data		

UO ₂ 1.6wt% Asm.	UO ₂ 2.4wt% Asm.	UO ₂ 3.1wt% Asm.
-----------------------------------	-----------------------------------	-----------------------------------

Fig. 3. Calculation result of axially-integrated detector signals using MVP-3b, and difference between original and tilt-corrected measurement data (top value: calculation results of MVP-3b with exact resonance scattering model, middle value: difference between calculation results and original (not corrected) measurement data, bottom value: difference between calculation results and tilt-corrected measurement data).

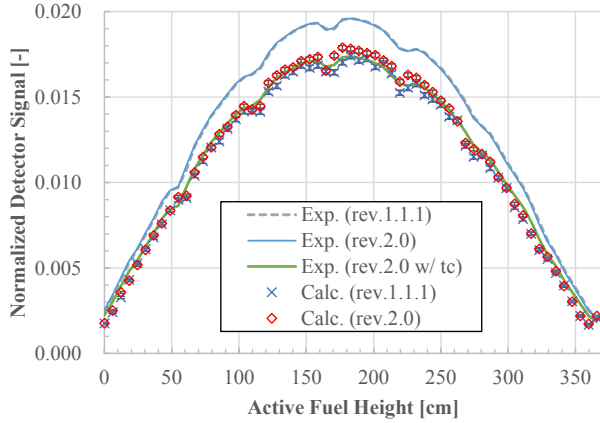


Fig. 4. Comparison of axial distribution at assembly B13 (vertical values are normalized by sum of all measurement data, and “w/ tc” means “tilt-corrected”)

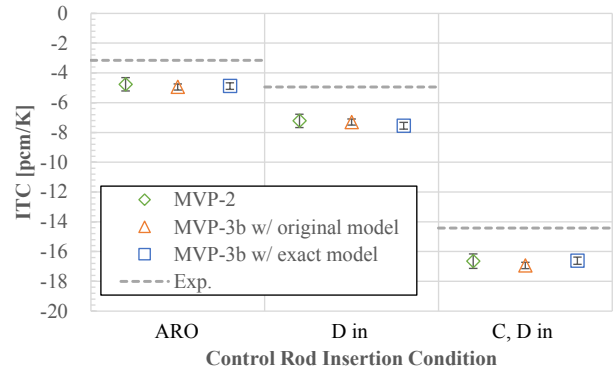


Fig. 7. Calculation results of ITC for each code version

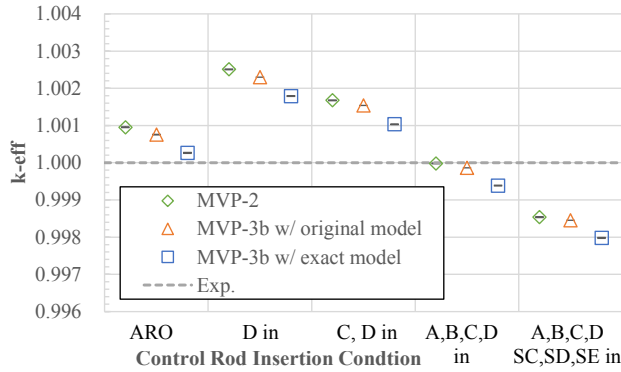


Fig. 5. Calculation results of criticality for each code version

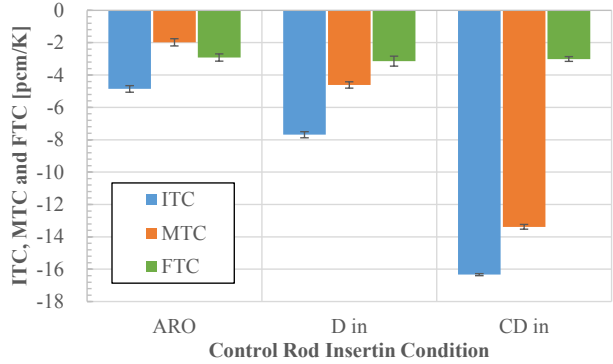


Fig. 8. Calculation results of ITC, MTC and FTC from each initial seed conditions (using revision 1.1.1 model)

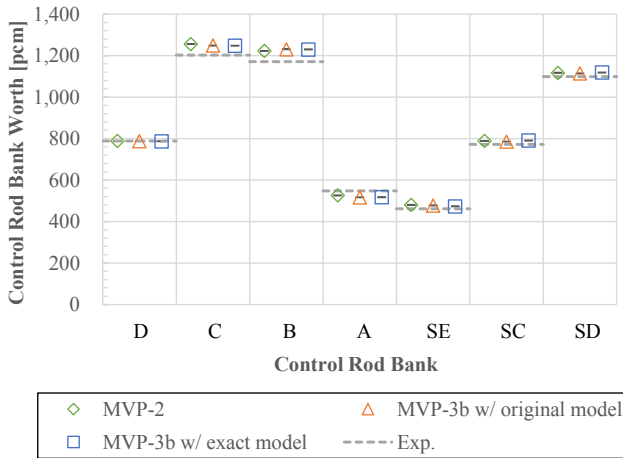


Fig. 6. Calculation results of control rod bank worth for each code version

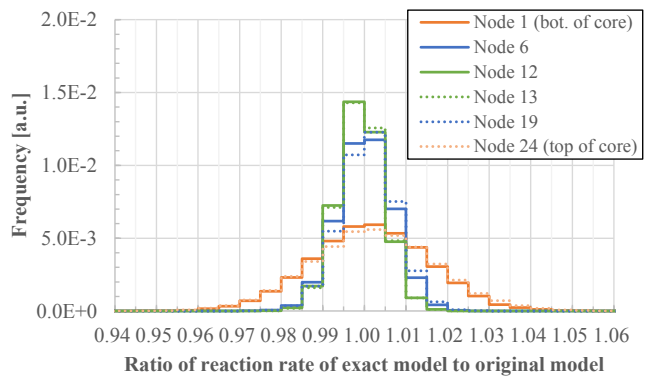


Fig. 9. Deviation of calculated fission reaction rate of exact model to original model (using revision 1.1.1 model)

IV. CONCLUSIONS

With the release of the updated BEAVRS benchmark model, modification points were reflected to whole core

calculation model for MVP calculation. The initial startup tests of the HZP condition were calculated using the latest version of MVP code with the nuclear data library based on JENDL-4.0. The calculation results of the criticality, the control rod bank worth, ITC and the in-core detector signals that corresponds to the thermal neutron flux distribution are discussed through two insights, an effect of the benchmark model and the code update. In the comparisons between the benchmark model revision 1.1.1 and 2.0, the results of the criticality and the control rod bank worth for both models can give good accuracy within the criteria in the standard [14]. On the other hand, the difference between models have tens pcm due to the specification updates. The thermal neutron flux distribution evaluated by in-core detector signals is well improved with the update of the benchmark model. The tilt-corrected data in revision 2.0 improved the results that have a large discrepancy at the outer of the core region in revision 1.1.1. In the comparison between code versions, the criticality slightly goes down, and the control rod bank worth, ITC, in-core detector signals varies little. From these comparisons, MVP-3b with the exact model would give good results while maintaining the calculation accuracy of MVP-2, and can also provide accurate results for the experiment data in HZP condition. The results contribute verification and validation for the latest version of MVP.

ACKNOWLEDGMENTS

Authors would like to thank Dr. Kenya Suyama and Dr. Yasunobu Nagaya of JAEA for providing MVP-3 beta version.

REFERENCES

1. Y. NAGAYA, K. OKUMURA, T. MORI, et al., "MVP/GMVP II: General Purpose Monte Carlo Codes for Neutron and Photon Transport Calculations based on Continuous Energy and Multigroup Methods", JAERI-1348, Japan Atomic Energy Research Institute (2005).
2. M. NAKAGAWA, T. MORI, "Whole Core Calculations of Power Reactors by Use of Monte Carlo Method", *J. Nucl. Sci. Technol.*, **30**, 7, 692 (1993).
3. M. TOHJOH, Y. ITOH, S. KATO, et al., "Applying the Monte-Carlo-Code "MVP-BURN" to BWR core analyses (4) -Full Core Analyses of Fresh Core-", *Proc. of 2004 Fall Meeting of AESJ*, Kyoto, Japan, Sep. 15-17, p.207, Atomic Energy Society of Japan (2004).
4. M. SUZUKI, Y. NAUCHI, "Analysis of BEAVRS Benchmark Problem by Using Enhanced Monte Carlo Code MVP with JENDL-4.0", *Proc. M&C+SNA+MC2015*, Nashville, Tennessee, Apr. 19-23, 2015, American Nuclear Society (2015) (CD-ROM).
5. T. MORI, Y. NAGAYA, "Comparison of Resonance Elastic Scattering Models Newly Implemented in MVP Continuous-Energy Monte Carlo Code", *J. Nucl. Sci. Technol.*, **46**, 8, 793 (2009).
6. Y. NAGAYA, K. OKUMURA, T. MORI, "Recent developments of JAEA's Monte Carlo code MVP for reactor physics applications", *Annals of Nuclear Energy*, **82**, 85 (2015).
7. N. HORELIK, B. HERMAN, B. FORGET, K. SMITH, "Benchmark for Evaluation and Validation of Reactor Simulations (BEAVRS)", *Proc. M&C 2013*, Sun Valley, Idaho, May 5-9, 2013, p.2986, American Nuclear Society (2013) (CD-ROM).
8. D. J. KELLY, B. N. AVILES, P. K. ROMANO, et al., "Analysis of Select BEAVRS PWR Benchmark Cycle 1 Results Using MC21 and OpenMC", *Proc. PHYSOR2014*, Kyoto, Japan, Sep. 28-Oct. 3, 2014, (CD-ROM).
9. M. RYU, Y. S. JUNG, H. H. CHO, et al., "Solution of the BEAVRS Benchmark Using the nTRACER Direct Whole Core Transport Code", *Proc. PHYSOR2014*, Kyoto, Japan, Sep. 28-Oct. 3, 2014, (CD-ROM).
10. B. COLLINS, A. GODFREY, "Analysis of the BEAVRS Benchmark Using VERA-CS", *Proc. M&C+SNA+MC2015*, Nashville, Tennessee, Apr. 19-23, 2015, American Nuclear Society (2015) (CD-ROM).
11. N. HORELIK, B. HERMAN, M. ELLIS, et al., "Benchmark for Evaluation and Validation of Reactor Simulations (BEAVRS), Release rev.2.0", MIT Computational Reactor Physics Group (2016).
12. K. SHIBATA, O. IWAMOTO, T. NAKAGAWA, et al., "JENDL-4.0: A New Library for Nuclear Science and Engineering", *J. Nucl. Sci. Technol.*, **48**, 1, 1 (2011).
13. K. OKUMURA, Y. NAGAYA, "Production of Neutron Cross Section Library Based on JENDL-4.0 to Continuous-energy Monte Carlo Code MVP and Its Application to Criticality Analysis of Benchmark Problems in the ICSBEP Handbook", JAEA-Data/Code 2011-010, Japan Atomic Energy Agency (2011).
14. "Reload Startup Physics Tests for Pressurized Water Reactors", ANSI/ANS-19.6.1-2011, American Nuclear Society, La Grange Park, IL, USA (2011).
15. D. J. KELLY, B. N. AVILES, B. R. HERMAN, "MC21 Analysis of the MIT PWR Benchmark: Hot Zero Power Results", *Proc. M&C 2013*, Sun Valley, Idaho, May 5-9, 2013, American Nuclear Society (2013) (CD-ROM).
16. Y. NAGAYA, "Monte Carlo Analysis of Doppler Reactivity Coefficient for UO₂ Pin Cell Geometry", *Proc. PHYSOR2014*, Kyoto, Japan, Sep. 28-Oct. 3, 2014, (CD-ROM).
17. T. YAMAMOTO, T. SAKAI, "Analysis of Temperature Effects on Reactivity of Light Water Reactor Fuel Assemblies by Using MVP-2 Adopting an Exact Resonance Elastic Scattering Model", *Proc. M&C+SNA+MC2015*, Nashville, Tennessee, Apr. 19-23, 2015, American Nuclear Society (2015) (CD-ROM).